ISSN 1062-3590, Biology Bulletin, 2021, Vol. 48, Suppl. 1, pp. S185–S196. © Pleiades Publishing, Inc., 2021.
Russian Text © The Author(s), 2019, published in Zoologicheskii Zhurnal, 2019, Vol. 98, No. 10, pp. 1100–1111.

Variability and Morphological Features of Woolly Rhinoceros Skulls (*Coelodonta antiquitatis* (Blumenbach 1799)) from Northeastern Asia in the Late Pleistocene

A. Y. Puzachenko[a, *], I. V. Kirillova[b, **], F. K. Shidlovsky[b, **], and V. A. Levchenko[c, *]**

[a] *Institute of Geography, Russian Academy of Sciences, Moscow, 119017 Russia*
[b] *NASH Ice Age Ltd., Moscow, 129223 Russia*
[c] *Australian Nuclear Science and Technology Organisation, Lucas Heights NSW 2234, Australia*
**e-mail: puzak@igras.ru*
***e-mail: ikirillova@yandex.ru*
****e-mail: vld@ansto.gov.au*

Received February 20, 2019; revised March 15, 2019; accepted March 20, 2019

Abstract—We studied 63 woolly rhinoceros skulls from the northeast of Russia (northwestern Chukotka, northeastern Yakutia) housed in the collection of the "Ice Age" Museum-Theatre, Moscow. Both sexual dimorphism and size/shape variability of woolly rhinoceros skulls are explored using univariate and multivariate statistics for the first time. Peculiarities of the variability, which are probably related to gender, are expressed in (1) different sets of skull variables the variability of which does not depend on "general size" variations and (2) differences in skull allometry in males and females. The structure of morphological variability is discussed. Statistically significant morphological heterogeneity is detected within the male and female samples. This is shown to be the consequence of the presence of two size groups that are not related to individual age. Based on published radiocarbon dates, it is hypothesized that there was a decrease in skull size in the woolly rhinoceros is at the end of megainterstadial (MIS) 3 to the early Last Glacial Maximum MIS 2 in northeastern Asia. To test this hypothesis, new radiocarbon dates of the studied specimens are needed.

Keywords: Pleistocene, Northeast Asia, *Coelodonta antiquitatis*, skull
DOI: 10.1134/S1062359021140144

Woolly rhinoceros (*Coelodonta antiquitatis (*Blumenbach 1799)) is a unique representative of the Mammuthus–Coelodonta faunistic complex of the Late Pleistocene of Eurasia (Kahlke, 2014), the representatives of which were well adapted to the harsh ecological conditions of the Würm (=Vistula =Valdai = Yermakov =Sartan) glaciation of northern Eurasia, corresponding to marine oxygen isotopes MIS 5d–MIS 2 (~110–12 ka ago). The area of origin of the woolly rhinoceros genus is believed to have been in the west of the modern Tibetan plateau (Deng et al., 2011). In the Middle Pliocene, about 3.7 million years ago, an early representative of the genus—*C. thibetana* Deng et al. 2011—lived here in a mountainous steppe landscape. Evidence of the subsequent expansion of woolly rhinoceros in Asia has been preserved in China, Mongolia, Transbaikalia and in the south of Western Siberia (de Chardin, Piveteau, 1930; Chow, Chow, 1959; Kahlke, 1969; Li, 1984; Zheng, Cai, 1991; Foronova, 1999; Deng et al., 2011). At the beginning of the Middle Pleistocene, about 460 ka ago (MIS 12), rhinoceros similar to *C. tologoijensis* Beliajeva 1966 appeared in Western Europe (Kahlke, Lacombat, 2008).

On the territory of Yakutia, woolly rhinoceros were probably absent until the Middle Neopleistocene (Sher, 1971; Lazarev, 2005; Kahlke, Lacombat, 2008). In the Late Pleistocene, this species was widespread in Eurasia from the Iberian Peninsula and the British Isles to Chukotka and Kamchatka (Markova et al., 2011; Stuart, Lister, 2012). The latest, early Holocene remains of a woolly rhinoceros were found in the Urals, in Lobvinskaya Cave, 9500 ± 250, IERZ-92 (Kosintsev, 1995).

The "Ice Age" Museum (Moscow) contains a significant collection of woolly rhinoceros skulls from the northeast of the Sakha republic (Yakutia) and northwest of the Chukotka autonomous okrug (Fig. 1). The volume of material made it possible to carry out a comprehensive study of the morphological variability of this regional "chronopopulation" of rhinoceroses that lived in the late Pleistocene in the western part of Beringia.

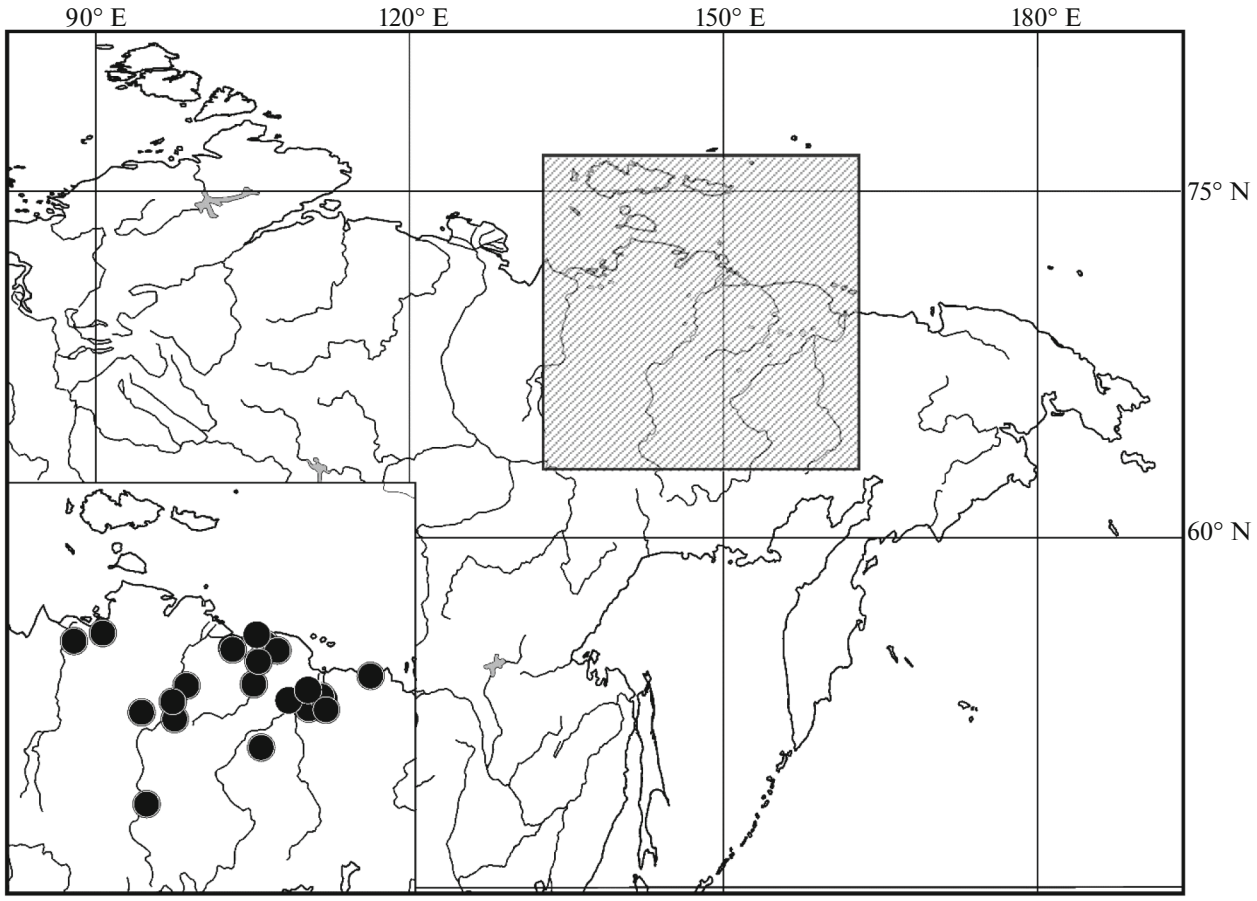

Fig. 1. Locations of the investigated woolly rhinoceros skulls.

MATERIALS AND METHODS

We examined 63 skulls of adult woolly rhinoceroses stored in the collection of the Ice Age Museum and collected on the territory of northeastern Yakutia and northwestern Chukotka (Fig. 1) in the basins of the Yana, Indigirka, Alazeya, Kolyma, etc., rivers.

The few available datings of the skulls included in the studied sample suggest that the age of the finds is mainly within the MIS 3 mega-interstadial (57–29 ka ago) and the beginning of the MIS 2 glaciation maximum (29–20 ka ago) (Lorenzen et al., 2011): 50097 ± 1047 (OxA-15915), 49940 ± 1160 (OxA-15731), 49310 ± 500 (OxA-15914), 48020 ± 740 (OxA-16324), 36290 ± 270 (OxA-16323), and 28700 ± 130 (Ox -15911) (hereinafter, radiocarbon dates are calibrated with OxCAl 4.3 software package and IntCal13 calibration curve (Ramsey, Lee, 2013).

The skulls were measured three times using a measuring table and two electronic calipers, ShTsTs-1-300 and ShTsTs-1-500, with an accuracy of 1 mm. We used the rhinoceros skull measurement technique proposed in (Guérin, 1980; van der Made, 2010) with additions (Fig. 2).

The age of the animals was assessed according to the qualitative characteristics of the skull: overgrowth of sutures, development of muscle attachment sites and the degree of eruption and wear of teeth, "maturity" of compact tissue; only skulls belonging to adults (ad), middle-aged (ad-mat), mature (mat), and senile (mat-sen) individuals were selected for the study. To assess the potential effect of age on the analysis results, we used correspondence analysis (Shafir, 2009; Beh and Lombardo, 2014) and the nonparametric Kruskal–Wallis test (Sokal and Rohlf, 1981).

Determination of the sex of the skull was carried out visually, on the basis of external signs: massiveness (length-to-width ratio) of the skull; the degree of development of muscle attachment points, including the occipital crest; the degree of development of roughness on the surface of the skull; and the width in the zygomatic arches. For some specimens, gender was determined, redefined, or confirmed by morphometric analysis. For this, we used part of a sample of skulls in which sex was determined with a high degree of confidence. This subsample was considered as "training" in the stepwise discriminant analysis. The belonging of the remaining specimens was assessed by the magnitude of the posterior probabilities. The man-

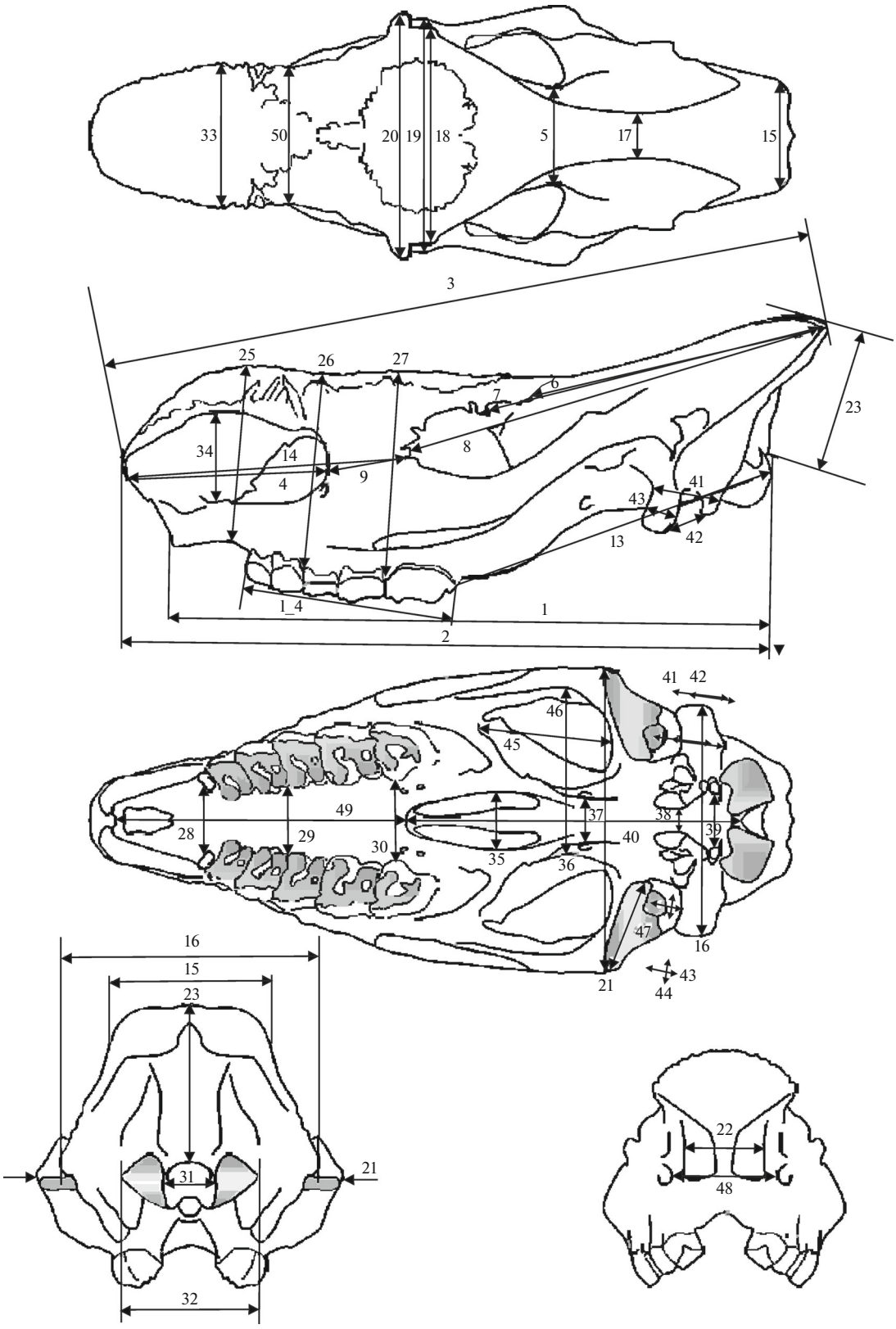
33
50
20
19
18
5
17
15
3
25
26
27
6
7
8
23
34
14
4
9
41
43
42
13
1_4
1
2
41
42
46
45
49
37
38
39
28
29
30
35
36
40
47
16
21
43
44
16
15
23
31
21
32
22
48

Fig. 2. Skull measurement scheme for woolly rhinoceros according to (van der Made, 2010). In our work, we used the following measurements: (*2*) the distance from the anterior edge of the nasal bones to the posterior surface of the occipital condyles, (*3*) the distance from the anterior edge of the nasal bones to the occiput, (*4*) the length of the nasal notch, (*5*) the minimum width of the postorbital region, (*6*) the distance from the postorbital process to the occiput, (*7*) the distance from the supraorbital process to the occiput, (*8*) the distance from the preorbital process to the occiput, (*9*) the distance from the notch between the nasal and intermaxillary bones (nasoincisive notch) to the anterior edge of the orbit, (*13*) the distance from the posterior edge of M3 to the posterior edge of the occipital condyle, (*14*) the distance from the anterior edge of the nasal bones to the anterior edge of the orbit, (*15*) the width of the occiput, (*16*) the width of the skull in the mastoid processes, (*17*) the minimum distance between the frontoparietal ridges, (*18*) the width between the postorbital processes, (*19*) the width between the supraorbital processes, (*20*) the width between the preorbital processes, (*21*) the maximum zygomatic width, (*22*) the width of the entrance to the nasal cavity, (*23*) the distance from the occipital foramen to the occipital crest, (*28*) the width of the palate measured in front of P2, (*29*) the width of the palate between P4 and M1, (*30*) the width of the palate measured in front of M3, (*31*) the width of the occipital foramen, (*32*) the width between the outer edges of the occipital condyles, (*33*) the width of the nasal bones, (*34*) the height of the nasal opening, (*35*) the width between the choanas, (*37*) the distance between the caudal wing openings (foramen alare caudal), (*38*) the distance between the lacerated openings (foramen lacerum), (*39*) the distance between the hyoid foramen (foramen nervi hypoglossi), (*45*) the length of the space inside the zygomatic arch, (*46*) the width of the space inside the zygomatic arch, (*47*) the width of the articular facet, (*48*) the distance between the infraorbital foramen, and (*50*) the minimum width of the nasal bones behind the region of origin of the nasal horn; I_4 is the length of the dentition.

ifestation of sexual dimorphism in individual measurements was assessed by the value of the sexual dimorphism index (Rossolimo, Pavlinov, 1974), which reflects the relative excess of the size of males over females.

The method for studying morphometric variability of the woolly rhinoceros skull has been previously tested on many objects (Puzachenko, 2001; Kupriyanova et al., 2003; Puzachenko, Zagrebelny, 2008; Abramov, Puzachenko, 2005; Abramov et al., 2009; 2016; Baryshnikov, Puzachenko, 2011 , 2017; Puzachenko et al., 2017, etc.). In the general case, the sequence of data analysis includes preparation of morphometric data (measurements), construction of a multidimensional model describing the main patterns of variability, and analysis of the results. The main purpose of data preparation is to eliminate the influence of measurement errors and fill in missing data. To search for "extreme values" and outliers, a visual method was used—the analysis of scatter diagrams and the Grubbs test (Stefansky, 1972). Values missing due to natural damage to the skull were filled using the EM algorithm (Dempster et al., 1977) and the regression method. To bring the initial measurements to the same scale, ranging was applied in accordance with the formula $x_{i,\text{rang}} = (x_i - x_{\min})/(x_{\max} - x_{\min})$. The construction of a multivariate model is aimed at a compact description of variability and identification of the main components of variability against the background of random variations ("noise"). The morphological space model is a Euclidean space, a small number of coordinates of which (virtual variables) contains basic information about the variation of many initial variables. Each object (skull) is represented in the model space by a point with coordinates that determine its geometric position relative to all other objects. To construct the morphological space, the method of nonmetric multidimensional scaling (NMDS) was used (Davison, Jones, 1983). As the initial data for this method, two matrices of "morphological distances" between all the skulls of the sample were calculated. The first matrix of pairwise standardized Euclidean distances mainly reflected the differences in the overall size of the skull. The corresponding model of the morphospace describes the dimensional variability and is designated as "morphospace of sizes" (model MSZ, designations of coordinates E1, E2, ..., etc.). The second variant of morphological distance estimation was obtained using Kendall's tau-b rank correlation (Kendall, 1975). The metric summarizes the differences in the shape/proportions of the skulls. The model corresponding to this metric is designated as the "morphospace of the shape" of the skull (model MSH, designation of coordinates K1, K2, ..., etc.) (Puzachenko, 2016). The optimal dimension of the morphospace (the number of coordinates) was estimated from the variation of the Kruskal stress index (Kruskal, 1964; Kupriyanova et al., 2003). Analysis of MSZ and MSH models included correlation analysis of the coordinates of the morphospace and initial measurements of the skull, in order to assess the quality and biological interpretation of the model; analysis of mixtures of Gaussian distributions (Gridgeman, 1970) in order to check the homogeneity of the distributions of coordinate values with statistical estimate by criterion *d* of Kolmogorov–Smirnov; and classification of the sample using coordinates as variables by the *k*-means method.

MSZ and MSH models were calculated both for the samples of putative males and females and for the entire sample as a whole. The corresponding coordinate models (GE1 and GK1) reproduce the variation in the generalized sizes and shapes of the skulls of rhinoceroses of both sexes.

For statistical data processing, we used STATISTICA v. 8.0 (StatSoft, Tulsa, Oklahoma, United States), PAST v. 3.12 (Hammer et al., 2001) and NCSS 12 Statistical Software (ncss.com/software/ncss).

Table 1. Measurements of the skull of a woolly rhinoceros with a sexual dimorphism index from 7 to 12%

Measure	Measurement name	Average between measurement values in males and females, mm	Statistical significance according to the Mann–Whitney test: Z. *p*	Sexual dimorphism index, %
22	Width of the entrance to nasal cavity	8.4	4.52, <0.0001	12.1
33	Width of nasal bones	18.9	5.32, <0.0001	11.2
50	Minimum width of nasal bones behind horn-attachment area	14.1	5.48, <0.0001	9.3
19	Width in supraorbital processes	22.7	5.01, <0.0001	8.6
15	Occiput width	16.4	3.27, 0.001	7.4
20	Width in preorbital processes	23.4	5.16, <0.0001	7.8

Table 2. Maximum values of Pearson correlation coefficients for coordinates of morphospaces MR (E1–E4) and MF (K1–K4) with measurements of the male skull

Measure	E1	E2	E3	E4	Measure	K1	K2	K3	K4
2	**0.80**	–0.40	0.21	–0.11	3	**0.65**	0.31	0.42	–0.04
21	**0.79**	0.27	–0.22	–0.17	8	**0.64**	0.19	0.48	0.08
20	**0.78**	0.42	0.13	0.20	7	**0.62**	0.21	0.52	0.20
50	**0.75**	0.24	–0.15	0.07	17	**–0.51**	–0.29	0.23	0.08
16	**0.73**	0.16	0.05	–0.25	35	**–0.52**	–0.06	0.06	–0.08
45	**0.72**	–0.37	0.03	–0.14	20	–0.32	**0.69**	0.30	0.15
33	**0.70**	0.04	0.01	0.10	18	–0.42	**0.66**	0.17	0.15
3	0.75	–0.54	–0.18	0.07	22	0.14	**0.63**	–0.08	–0.04
8	0.66	–0.59	–0.28	0.07	28	–0.07	**0.54**	–0.05	0.04
7	0.64	–0.57	–0.31	0.14	48	–0.07	**0.58**	–0.09	0.12
35	0.31	**0.55**	–0.25	–0.23	38	–0.19	0.01	**0.67**	0.18
48	–0.07	**0.58**	–0.09	0.12	6	0.48	0.08	**0.61**	0.17
37	0.48	0.32	**–0.57**	–0.23	37	–0.22	–0.10	**0.54**	–0.06
17	0.17	0.47	**–0.52**	–0.16	31	0.08	–0.25	–0.28	**–0.51**
38	–0.19	0.01	**0.67**	0.18	I_4	0.40	0.04	0.08	**0.52**
31	0.11	–0.08	–0.01	**–0.70**	4	0.45	0.17	–0.22	**–0.51**

Values of measurements that form the basis of skull variability are marked in bold.

RESULTS

Sexual Dimorphism of the Skull

In most measurements of the skull of the woolly rhinoceros, the putative sexual dimorphism is insignificant and manifests itself on parts of the skull that are directly or indirectly associated with the attachment of the anterior and posterior horns and with the width of the occiput (Table 1). The horns of the males probably had more powerful and wider bases. The largest difference (12–11%) between males and females was determined for the width of the entrance to the nasal cavity and the width of the nasal bones (measurements 22 and 33).

Sexual dimorphism is poorly expressed in the overall dimensions of the skull, such as condylobasal length or maximum width in the zygomatic arches.

Despite the obtained evidence of a low contribution of sexual dimorphism, this factor can influence the results of morphometric analysis. Therefore, further samples of males (38 skulls) and females (25 skulls) were analyzed separately.

Structure of Cranial Variability

The morphological spaces of males had a dimension of four; for females, three (MSZ) and five (MSH), respectively. The Kruskal–Wallis test and the analysis of correspondences did not reveal the influence of the belonging of an individual age on the values of the coordinates of the models.

In males, the maximum values of the Pearson correlation coefficient with the first coordinate E1 were

Table 3. Maximum values of Pearson correlation coefficients for coordinates of morphospaces MSZ (E1–E3) and MSH (K1–K5) with measurements of the female skull

Measure	E1	E2	E3	Measure	K1	K2	K3	K4	K5
3	**0.91**	–0.15	0.25	I_4	**0.78**	0.01	0.28	0.14	-0.12
8	**0.89**	–0.16	0.18	7	**0.70**	0.39	–0.03	–0.04	–0.23
2	**0.85**	0.03	0.30	8	**0.69**	0.41	–0.13	–0.06	–0.19
6	**0.84**	–0.10	0.23	3	**0.62**	0.36	–0.16	–0.03	–0.14
45	**0.83**	–0.01	0.05	18	–0.25	**0.77**	0.03	–0.02	0.06
7	**0.82**	–0.26	0.12	19	–0.29	**0.74**	0.19	–0.15	–0.30
50	**0.78**	–0.15	–0.18	20	–0.04	**0.66**	0.25	0.13	–0.09
14	**0.78**	–0.03	–0.03	39	–0.12	-0.03	**–0.62**	0.08	0.02
23	**0.74**	–0.22	–0.11	29	0.32	0.13	**0.53**	0.19	0.16
5	**0.73**	0.27	0.26	37	0.14	0.26	–0.27	**0.67**	–0.09
17	**0.70**	0.11	0.10	38	0.10	0.31	–0.03	**0.52**	–0.31
4	**0.67**	0.05	0.08	31	–0.43	-0.06	-0.02	-0.25	**-0.60**
I_4	0.70	–0.58	–0.05						
33	0.66	–0.20	–0.43						
35	0.05	**0.86**	0.01						
13	0.25	**0.69**	0.02						
18	0.33	**0.64**	–0.16						
19	0.39	**0.62**	–0.37						
39	0.19	0.06	**0.59**						

Values of measurements that form the basis of skull variability are marked in bold.

obtained for the condylobasal length ($r = 0.80$), width in the zygomatic arches ($r = 0.79$), width in the preorbital processes ($r = 0.78$), and a number of other features (Table 2). The E2 coordinate correlates with the width between choanas ($r = 0.55$), and the distance from the supraorbital and preorbital processes corresponds to the occiput ($r = –0.59, –0.57$). Specific measurements correlating with the E3 coordinate are the distance between the caudal foramen (measurement 37) and the distance between the frontoparietal ridges (measurement 17), while the width of the foramen magnum correlates with the E4 coordinate.

Measurements that correlate predominantly or only with one of the coordinates of the model form an "orthogonal" basis for the variability of the skull. These measurements that determine the dimension of the morphospace.

The correlation of measurements with the MSH coordinates is lesser in magnitude (Table 2). Since the coordinates in this case reproduce the variability of the proportions of the skull, then for measurements that correlate primarily with the K1 coordinate, allometric variability is likely (measurements of the skull length associated with the occiput, the minimum distance between the frontoparietal ridges, and the width between the choanas). In addition to the listed measurements, the bases for the variability of the proportions of the skull of males includes the length of the dentition, the width of the skull between the preorbital and postorbital processes, and the width of the entrance to the nasal cavity (Table 2).

Analysis of the coordinates of MSZ and MSH of male models showed that the sample is heterogeneous and the distribution of the values of the E1 coordinate is probably bimodal (criterion d of Kolmogorov–Smirnov = 0.084, $p = 0.93$, Fig. 3a). In other words, the sample may contain two groups of skulls with different mean skull sizes. The subsequent dichotomous classification according to the values of the coordinates of the MSZ model divided the sample into two groups of skulls (Fig. 3b). Representatives of different size groups did not practically differ in the proportions of the skull (Fig. 3c). According to the Mann–Whitney test, the largest significant differences ($p < 0.001$) between groups characterize the distance from the tip of the nasal bones to the occiput, the distance from the tip of the nose to the anterior border of the orbit, the maximum width in the zygomatic arches, the width of the skull in the mastoid processes, the width of the nasal bones, and other characteristics. There were no differences between the size groups in terms of measurements: the minimum distance between the frontoparietal ridges, the width of the foramen magnum, the length of the dentition, and a number of other measurements that do not correlate with the E1 coordinate. Using the analysis of correspondences, it was not

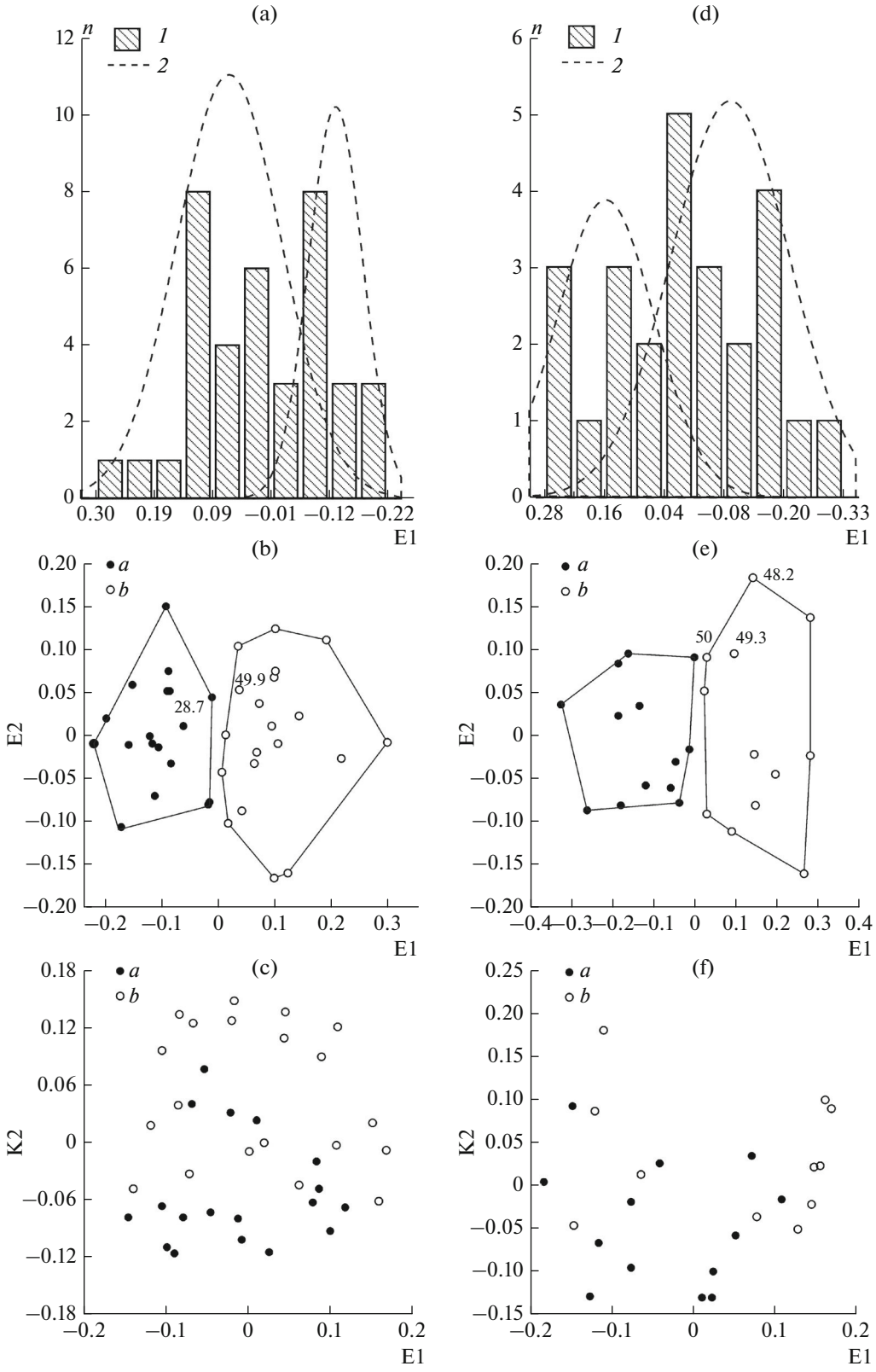

Fig. 3. Size groups of woolly rhinoceros skulls in MSZ and MSH models. (a, d) (*1*) empirical frequency distribution (n) of the values of the first coordinate of MSZ models (E1), which correlates with the total size of the woolly rhinoceros skull, and (*2*) the model of a "mixture" of two Gaussian distributions for samples of (*A*) males and (*D*) females; (b–f) distribution of specimens of skulls of (b, c) males and (e, f) females relative to the first two coordinates of the (b, e) MSZ and (c, f) MSH models, (*1*) group with small skulls, (*2*) group with large skulls, numbers in diagrams *b* and *e* indicate the geological age of the specimen, ka.

possible to detect the influence of the individual age of animals on the composition of size groups.

The variability in the size of the skull of the putative female woolly rhinoceros looks more ordered, which is reflected in the lower dimension of the MSZ model and higher values of the correlation coefficients of coordinates with measurements (Table 3). The first coordinate (E1) here also describes the variation in the overall dimensions of the skull (its predominant length): the distance from the anterior edge of the nasal bones to the occiput and condylobasal length, the length of the space inside the zygomatic arch, and features. The E2 coordinate correlates with the width between the choanas and the distance from the posterior edge of M3 to the edge of the occipital condyle. The distance between the hyoid foramen is an indicator measurement of the E3 coordinate.

The dimensionality of the MSH model in females is higher than in males (Table 3). As in males, the K1 coordinate correlates with measurements related to the occipital region of the skull, but in this case the length of the dentition is added to them. As in males, in females the proportions of the skull width in the orbital region are reproduced by the K2 coordinate. The K3 coordinate, which is unique to females, correlates with the distance between the hyoid foramen and the width of the palate at the P4–M1 level (measurement 29). The K4 coordinate correlates with a specific measurement—the width between of foramen alare caudal. Finally, the K5 coordinate reproduces the variation in the relative width of the foramen magnum.

The distribution of the values of the E1 coordinate in females also turned out to be bimodal (Kolmogorov–Smirnov $d = 0.073$, $p = 0.99$, Fig. 3d). The scatter diagrams in coordinates E1–E2 and K1–K2 (Figs. 3e, 3f) demonstrate that the two groups differ from each other only in the overall size of the skull. They differ to the greatest extent in the distance from the supraorbital process to the occiput, the distance from the postorbital process to the occiput, the distance from the anterior edge of the nasal bones to the occiput, the distance from the preorbital process to the occiput, the minimum width of the nasal bones behind the nasal horn attachment area, and the minimum distance between frontoparietal ridges. The use of the matching analysis method did not reveal the influence of the estimated individual age on the size of the skull measurements in female rhinoceroses from different size groups.

Figure 4a shows the regression lines of the E1 coordinates of MSZ models relative to the GE1 coordinates (E1 = a + b * GE1) for males and females from different size groups. Formally, the differences between males and females are expressed in different slopes of the E1 regression lines relative to the GE1 abscissa axis. In this case, allometric variability suggests that in the group including large skulls, sexual dimorphism in overall size should be more pronounced than in the group with small skulls.

In the variability of the proportions of the skull of males and females (coordinates K1 and GK1, Fig. 4b), differences between the sexes are also present, but are much less pronounced. The K1 coordinates of both sexes correlate with measurements related to the length of the skull and the relative length of its cerebral region (Tables 2, 3). The GK1 coordinate of the MSH model, which includes both sexes, also correlates with the distance from the supraorbital process to the occiput normalized to the distance from the anterior edge of the nasal bones to the occiput (Fig. 4c). In females, this dependence is more clearly expressed (Pearson's correlation coefficient $r = 0.54$, $p = 0.005$). In addition (see Table 3), in females, compared with males, the variability of the relative length of the dentition is limited (Fig. 4d). In females, GK1 correlates with the length of the dentition normalized to the distance from the anterior edge of the nasal bones to the occiput, with a correlation coefficient of 0.61 ($p = 0.001$), while there is no such correlation in males. Belonging to one of the two size groups, apparently, does not affect the proportions of the skull (Fig. 4b).

DISCUSSION

Sexual Dimorphism

Sexual dimorphism is known in both modern and fossil rhinoceros (Mihlbachler, 2005; Chen et al., 2010), although it is less pronounced than in other mammals. Adult males and females differ morphologically in several ways. For example, male Indian rhinoceros (*Rhinoceros unicornis* L. 1758) have longer mandibular incisors (but not horns), more powerful muscles of the neck and shoulders, and extensive folds of the neck and shoulder, which is important when fighting for females during the breeding season (Dinerstein, 1991). Dimorphism is more pronounced in captive animals. Males are significantly taller at the withers and greater in body weight (up to 1000 kg) than in nature, which is explained by the lack of competition between males in zoos. In nature, severe stress and poor nutrition during a long nonbreeding interval, when young males are driven from productive pastures by dominant males, cause equalization of sizes (Dinerstein, 1991).

For the Miocene *Chilotherium wimani* Ringström 1924 male, the features are considered to be the long second incisor, the long molars, the greater height and length of the occipital part of the skull (Chen et al., 2010). The specified author reviewed the gender differences in modern rhinoceroses according to the literature and noted their variability for different species: in the Javanese and Sumatran rhinoceroses, sexual dimorphism manifests itself more in the incisors than in the size of the body and horns, while the black rhinoceros is monomorphic; sexual dimorphism in the

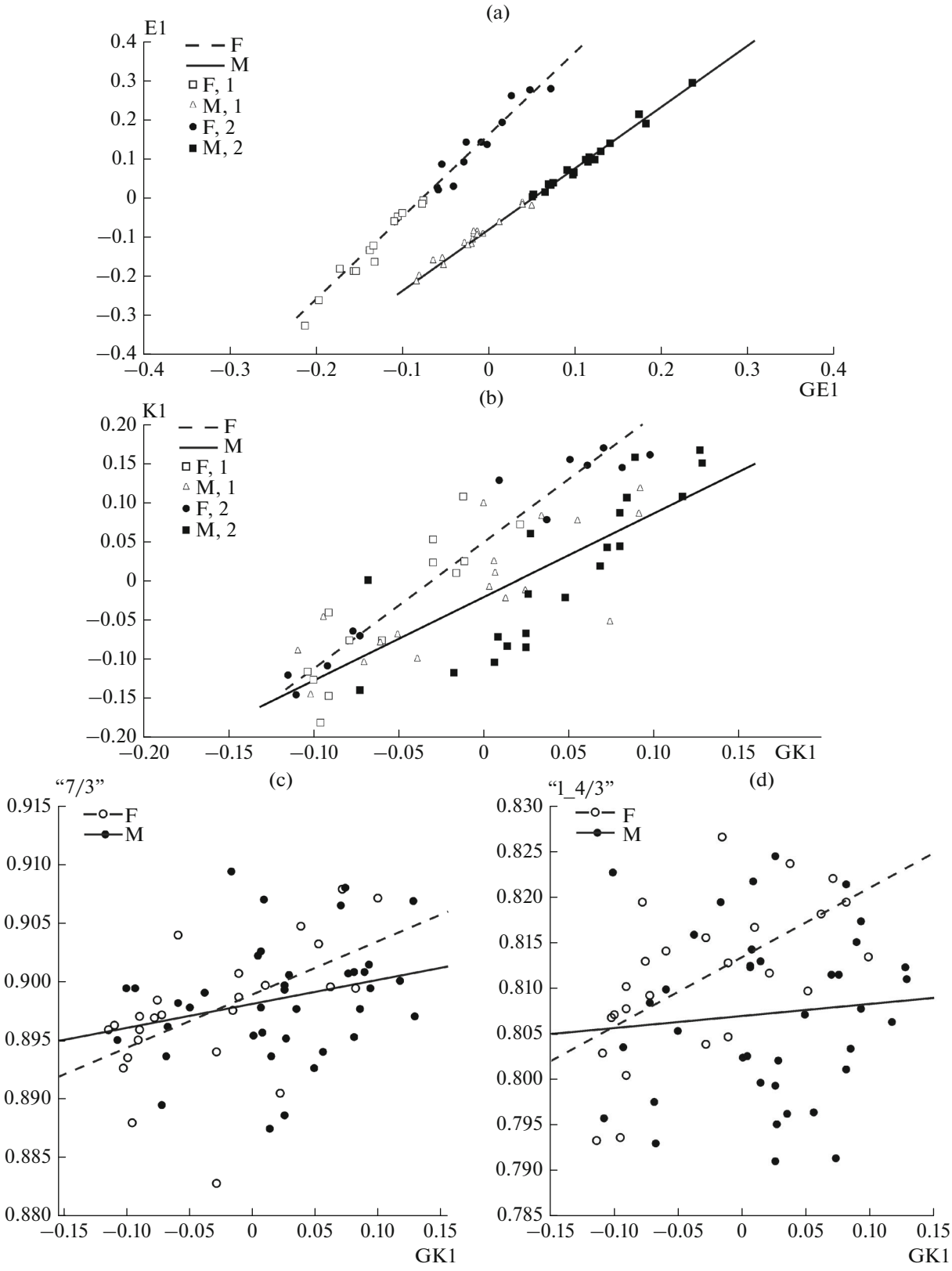

Fig. 4. Allometric variability in two size groups of woolly rhinoceros skulls. (a, b) allometric patterns of (a) general sizes and (b) proportions of skulls of females (F) and males (M) woolly rhinoceroses belonging to two size groups, in coordinates of MSZ (E1) and MF (K1) models and similar models for both sexes (GE1, GK1) (*1*, group with small skulls, (*2*) group with large skulls); (c, d) diagrams illustrating the relationship between changes in the first coordinate of the MSH model for males and females (GK1) with the relative distance from the supraorbital process to the occiput ("7/3") and the relative length of the dentition ("I_4/3").

white rhinoceros (*Ceratotherium simum* (Burchell 1817)) is expressed in horn size, body weight, and the neck; adult males of white rhinoceros are 25–43% heavier than females.

Gender differences in adult woolly rhinoceros are "incomplete" and rather weakly expressed (Borsuk-Bialynicka, 1973). According to this author, sexual dimorphism in a sample from one population is manifested only in extreme values of the distributions of traits. Despite the significant overlap in the distributions of traits in males and females, males are distinguished by a greater length of the skull and a greater zygomatic and orbital width of the skull. The distance from the occipital crest to the orbit and the widths of the occiput and nasal bones do not show a clear bimodality of the distributions, which may be associated with individual variability (Borsuk-Bialynicka, 1973).

Our study showed that the putative sexual dimorphism of different dimensions of the woolly rhinoceros skull varies within the range of 0–12.1%. In general, it was noted that the differences between the sexes are small. These differences are most clearly manifested in the rostral and supraorbital regions of the skull and are most likely associated with dimorphism in the sizes of the anterior and posterior horns. The roughness of individual bone structures also varies greatly—from weak to extremely pronounced, usually in males. In the second case, its development can be associated with a high hormonal status.

Sexual dimorphism manifested itself not only in the average values of measurements, but to a much greater extent in the structure of variability in the size and proportions of the skull. The data presented demonstrate both a similarity of the basis of variability of both sexes and their noticeable differences. The latter are manifested in different dimensions of morphospaces and sets of measurements that form the basis of variability. In males, the group of measurements, the values of which depend on the total size of the skull (correlate with the E1 coordinate), include mainly measurements of the total length and width of the skull. In females, a similar group of measurements also includes measurements characterizing the occipital region of the skull. In males, these measurements simultaneously correlate with both the first and second coordinates of the MSZ model (Tables 1, 2); i.e., their final values depend on two independent ontogenetic factors. Variations in the development of the occipital skull significantly affect the overall proportions of the skull in both sexes, which is reflected in the structure of the MSH models.

Hypothesis of a Change in the Size of the Skull of Woolly Rhinoceroses at the End of the Late Pleistocene (Second Half of MIS 3 to MIS 2)

In this study of woolly rhinoceros skulls, against the background of relatively weak sexual dimorphism in overall size, statistical methods were used to identify two size groups. The differences between "large" and "small" specimens are manifested mainly in overall size. A comparison of size-group belonging with the geological age of the skulls (Figs. 3b, 3e) allows us to make a cautious assumption that large skulls in the studied sample are often older, possibly more than 40 thousand radiocarbon years (MIS 3, MIS 4, or older). In this case, we can only say that there is a tendency ("trend"), and not a sharp change, in the size of animals at the end of the MIS 3 and the beginning of the MIS 2. This chronological hypothesis requires testing, for which it is necessary to obtain additional radiocarbon dates. It is also necessary to check how genetically similar "large" and "small" specimens are. At this stage of research, it is assumed that both morphological groups belong to the same haplotype or haplogroup of mtDNA. In this case, if the "chronological" hypothesis is confirmed, the decrease in the size of the skull can be associated with changes in the ecological living conditions of rhinoceros of the same chronopopulation that lived in this part of Northeastern Asia. To characterize changes in the nutritional spectrum of rhinoceroses, it is advisable to simultaneously evaluate the isotopic composition ($\delta^{13}C$, $\delta^{15}N$) skull bones from different size groups. According to an alternative hypothesis, a change in the rhinoceros population in the area under consideration took place in the second half of MIS 3.

ACKNOWLEDGMENTS

We are grateful to P.E. Kolesnikov for constructing the measuring table and G.P. Goncharova for technical assistance.

FUNDING

This paper was prepared on the topic of state assignment no. 0148-2019-0007 (AAAA-A19-119021990093-8) "Assessment of Physical-Geographical, Hydrological, and Biotic changes in the Environment and Their Consequences for Creating the Foundations of Sustainable Nature Management."

COMPLIANCE WITH ETHICAL STANDARDS

The authors declare that they have no conflicts of interest. This article does not contain any studies involving animals or human participants performed by any of the authors.

REFERENCES

Abramov, A.V. and Puzachenko, A.Y., Sexual dimorphism of craniological characters in Eurasian badgers, *Meles* spp. (Carnivora, Mustelidae), *Zool. Anzeiger—J. Comp. Zool.*, 2005, vol. 244, pp. 11–29.

Abramov, A.V., Puzachenko, A.Y., and Tumanov, I.L., Morphological differentiation of skull in two closely-related mustelid species (Carnivora, Mustelidae), *Zool. Stud.*, 2016, vol. 55, no. 1, pp. 1–23.

Abramov, A.V., Puzachenko, A.Y., and Wiig, O., Cranial variation in the European badger *Meles meles* (Carnivora, Mustelidae) in Scandinavia, *Zool. J. Linn. Soc*., 2009, vol. 157, pp. 433–450.

Baryshnikov, G.F. and Puzachenko, A., Craniometrical variability of cave bears (Carnivora, Ursidae): multivariate comparative analysis, *Quat. Int*., 2011, vol. 245, pp. 350–368.

Baryshnikov, G.F. and Puzachenko, A.Y., Morphometric analysis of metacarpal and metatarsal bones of cave bears (Carnivora, Ursidae), *Fossil Imprint*., 2017, vol. 73, pp. 7–47.

Beh, E.J. and Lombardo, R., *Correspondence Analysis: Theory, Practice and New Strategies*, Chichester: Wiley, 2014.

Borsuk-Bialynicka, M., Studies on the Pleistocene rhinoceros *Coelodonta antiquitatis* (Blumenbach), *Palaeontol. Pol*., 1973, no. 29.

Chen, S., Deng, T., Hou, S., Shi, Q., and Pang, L., Sexual dimorphism in perissodactyl rhinocerotid *Chilotherium wimani* from the Late Miocene of the Linxia Basin (Gansu, China), *Acta Palaeontol. Pol*., 2010, vol. 55, no. 4, pp. 587–597.

Chow, M. and Chow, B.S., Villafranchian mammals from Lingyi, S.W. Shansi, *Acta Palaeontol. Sin*., 1959, vol. 7, pp. 89–97.

Davison, M.L. and Jones, L.E., Special issue: multidimensional scaling and its applications, *Appl. Psychol. Meas*., 1983, vol. 7, pp. 373–514.

Dempster, A., Laird, N., and Rubin, D., Maximum likelihood from incomplete data via the EM algorithm, *J. R. Stat. Soc. Ser*., 1977, no. 1. Deng, T., Wang, X., Fortelius, M., Li, Q., Wang, Y., Tseng, Z.J., Takeuchi, G.T., Saylor, J.E., Saila, L.K., and Xie, G., Out of Tibet: Pliocene woolly rhinoceros suggests high plateau origin of ice age megaherbivores, *Science*, vol. 333, no. 6047, pp. 1285–1288.

Dinerstein, E., Sexual dimorphism in the greater one-horned rhinoceros (*Rhinoceros unicornis*), *J. Mammal*., 1991, vol. 72, pp. 450–457.

Foronova, I.V., Quaternary mammals and stratigraphy of the Kuznetsk Basin (south-western Siberia), *Anthropozoikum*, 1999, vol. 23, pp. 71–97.

Gridgeman, N.T., A comparison of two methods of analysis of mixtures of normal distributions, *Technometrics*, 1970, vol. 12, no. 4, pp. 823–833.

Guerin, C., Les rhinocéros (Mammalia, Perissodactyla) du Miocène terminal au Pléistocène supérieur en Europe occidentale; comparaison avec les espèces actuelles, *Doc. Lab. Géol. Lyon*, 1980, vol. 79, nos. 1–3, pp. 1–1185.

Hammer, Ø., Harper, D.A.T., and Ryan, P.D., PAST: paleontological statistics software package for education and data analysis, *Palaeontol. Electron*., 2001, vol. 4, pp. 1–9.

Kahlke, H.-D., Die Rhinocerotiden-Reste aus den Kiesen von Süßenborn bei Weimar, *Paläontol. Abh*., 1969, vol. A3, nos. 3/4, pp. 667–709.

Kahlke, R.-K., The origin of Eurasian mammoth faunas (*Mammuthus-coelodonta* faunal complex), *Quat. Sci. Rev*., 2014, vol. 96, pp. 32–49.

Kahlke, R.D. and Lacombat, F., The earliest immigration of woolly rhinoceros (*Coelodonta tologoijensis*, Rhinocerotidae, Mammalia) into Europe and its adaptive evolution in palaearctic cold stage mammal faunas, *Quat. Sci. Rev*., 2014, vol. 27, nos. 21–22, pp. 1951–1961.

Kendall, M.G., *Rank Correlation Methods*, London: Charles Griffin and Co., 1975.

Kosintsev, P.A., Remains of large mammals from the Lobvinskaya Cave, in *Materialy po istorii sovremennoi bioty Srednego Urala* (Materials on the History of Modern Biota of the Middle Urals), Bykov, G.V., Editor-in-Chief, Institute of Ecology, Ural Branch of the Russian Academy of Sciences, Yekaterinburg: Yekaterinburg, 1995, pp. 58–102.

Kruskal, B., Multidimensional scaling by optimizing goodness of fit to nonmetric hypothesis, *Psychometrika*, 1964, vol. 29, pp. 1–27.

Kupriyanova, I.F., Puzachenko, A.Yu., and Agadzhanyan, A.K., Temporal and spatial components of the variability of the skull of the common shrew, *Sorex araneus* (Insectivora), *Zool. Zh*., 2003, vol. 82, no. 7, pp. 839–851.

Lazarev, P.A., Large mammals of the Anthropogene of Yakutia (phylogeny, taxonomy, paleoecology, faunistic complexes, taphonomy, and remains), *Extended Abstract of Doctoral (Biol.) Dissertation*, Yakutsk: Institute of Applied Ecology of the North of the Academy of Sciences of the Republic of Sakha (Yakutia), 2005.

Li, Y., Fossil mammals and their stratigraphic age from Danangou, Yuxian Co., Hebei Province, *Vertebr. Palasiat*., 1984, vol. 22, pp. 60–68.

Lorenzen, E.D., Nogues-Bravo, D., Orlando, L., Weinstoc, J., Binladen, J., Marske, K.A., Ugan, A., Borregaard, M.K., Gilbert, M.T.P., Nielsen, R., Simon, Y.W.H., Goebel, T., Graf, K.E., Byers, D., Stenderup, J.T., Rasmussen, M., Campos, P.F., Leonard, J.A., Koepfli, K.-P., Froese, D., Zazula, G., Stafford, T.W., Aaris-Sorensen, K., Batra, P., Haywood, A.M., Singarayer, J.S., Valdes, P.J., Boeskorov, G., Burns, J.A., Davydov, S.P., Haile, J., Jenkins, D.L., Kosintsev, P., Kuznetsova, T., Lai, X., Martin, L.D., McDonald, H.G., Mol, D., Meldgaard, M., Munch, K., Stephan, E., Sablin, M., Sommer, R.S., Sipko, T., Scott, E., Suchard, M.A., Tikhonov, A., Willerslev, R., Wayne, R.K., Cooper, A., Hofreiter, M., Sher, A., Shapiro, B., Rahbek, C., and Willerslev, E., Species-specific responses of Late Quaternary megafauna to climate and humans, *Nature*, 2011, vol. 479, pp. 359–478.

van der Made, J., The rhinoceros from the Middle Pleistocene of Neumark-Nord (Saxony-Anhalt), *Veroffentlichungendes Landesamtes fur Denkmalpflegeund Archaologie*, 2010, vol. 62, pp. 433–500.

Markova, A.K. and Puzachenko, A.Yu., Kol'fskhoten van T., der Plikht van I., Ponomarev D.V., The latest data on the dynamics of the ranges of mammoth and woolly rhinoceros in Europe in the second half of the late Pleistocene–Holocene, *Izv. Ross. Akad. Nauk, Ser. Geogr*., 2011, no. 4, pp. 54–65.

Mihlbachler, M.C., Linking sexual dimorphism and sociality in rhinoceroses: insights from *Teleoceras proterum* and *Aphelops malacorhinus* from the late Miocene of Florida, *Bull. Florida Mus. Nat. Hist*., 2005, vol. 45, no. 4, pp. 495–520.

Puzachenko, A.Yu., Intrapopulation variability of the skull of the common mole rat *Spalax microphthalmus* (Spalacidae, Rodentia). 1. Methods of data analysis, non-aging variability of males, *Zool. Zh*., 2001, vol. 80, no. 3, pp. 1–15.

Puzachenko, A.Yu., *Kolichestvennye zakonomernosti morfologicheskogo raznoobraziya cherepa mlekopitayushchikh (Quantitative Patterns of Morphological Diversity of the Skull of Mammals)*, Pavlinov, I.Ya., Kalyakin, M.V., and Sysoev, A.V., Eds.,

Sb. Tr. Zool. Muz. Mosk. Gos. Univ., 2016, vol. 54, pp. 229–268.

Puzachenko, A.Yu. and Zagrebel'nyi, S.V., Variability of the skull of Arctic foxes *Alopex lagopus lagopus* (Carnivora, Canidae) of Eurasia, *Zool. Zh.*, 2008, vol. 87, no. 9, pp. 1106–1123.

Puzachenko, A.Y., Abramov, A.V., and Rozhnov, V.V., Cranial variation and taxonomic content of the marbled polecat *Vormela peregusna* (Mustelidae, Carnivora), *Mammal. Biol.*, 2017, vol. 83, pp. 10–20.

Ramsey, B.C. and Lee, Sh., Recent and planned developments of the program OxCal, *Radiocarbon*, 2013, vol. 55, pp. 720–730.

Rossolimo, O.L. and Pavlinov, I.Ya., Polovye razlichiya v razvitii, razmerakh i proportsiyakh cherepa lesnoi kunitsy (Martes martes L.: Mammalia, Mustelidae), *Byull. Mosk. O-va Ispyt. Prir.*, 1974, vol. 79, no. 6, pp. 23–35.

Shafir, M.A., Correspondence analysis: presentation of the method, *Sotsiologiya*, 2009, no. 28, pp. 20–44.

Sher, A.V., *Mlekopitayushchie i stratigrafiya pleistotsena severo-vostoka SSSR i Severnoi Ameriki* (Mammals and Stratigraphy of the Pleistocene of the Northeastern Ussr and North America), Moscow: Nauka, 1971.

Sokal, R.R. and Rohlf, F.J., *Biometry*, 2nd ed., New York: Freeman, 1981.

Stefansky, W., Rejecting outliers in factorial designs, *Technometrics*, 1972, vol. 14, no. 2, pp. 469–479.

Stuart, A.J. and Lister, A.M., Extinction chronology of the woolly rhinoceros *Coelodonta antiquitatis* in the context of Late Quaternary megafaunal extinctions in northern Eurasia, *Quat. Sci. Rev.*, 2012, vol. 51, pp. 1–17.

Teilhard de Chardin, P. and Piveteau, J., Les mammiferes fossiles de Nihowan (Chine), *Ann. Paleontol.*, 1930, vol. 19, pp. 1–134.

Zheng, S. and Cai, B., Micromammalian fossils from Danangou of Yuxian, Hebei, in *Contribution to INQUA XIII*, Beijing: Beijing Scientific and Technological Publishing House, 1991, pp. 100–131.